Chapter

Coordination Compounds of Lanthanides as Materials for Luminescent Turn Off Sensors

Claudio Pettinari, Andrei Drozdov and Yuriy Belousov

Abstract

This review aims at describing the possible use of lanthanide coordination compounds as materials for luminescent sensors now more necessary due to the continuous requirements from the society of electroluminescent and lighting devices, for example analytical sensors and imaging instruments. This is the first part of a work describing the photophysical foundations of the luminescence of complex compounds of lanthanides in the context of design materials with a sensory response, and also considers in detail materials with the most common type of response - *turn off* sensors.

Keywords: lanthanides, coordination compounds, luminescence, sensors, sensory response mechanism, turn off sensors

1. Introduction

The use of coordination compounds, organometallic and inorganic species containing lanthanides (Ln) as luminescent materials is mainly due to electronic transitions inside f-shells [1–6]. The design of luminescent sensors based on lanthanides is currently catching up and the number of papers on emitting materials, in particular Organic Light-Emitting Diode (OLED), is increasing. Several lanthanide complexes and Metal Organic Frameworks (MOFs) were described as useful for ratiometric fluorescent sensing [2] or potentially employable as functional materials [5]. These compounds are often characterized by switchable and tunable properties allowing fine-tuned optical features and sensitive responses to small molecules and ions. Several reviews [7–12] have reported lanthanide-containing luminescent sensor materials, which can be used for detecting anions [9] or low molecular weight analytes [8], and also for detecting cations [12]. The rapid growth in the number of publications requires a systematization that could help in the choice of the right compounds for new devices. Here we report a general overview of the principles governing the lanthanide coordination compounds luminescence and the most important examples of Ln compounds for sensing both ions and low molecular weight compounds. We have decided to report here a classification of the species based on the type of *sensory signal being recorded*, in detail "turn off", "turn on" and "ratiometric" sensors.

2. Lanthanide complexes luminescence principles

To understand how to control a sensory response by using a lanthanide complex as sensor material, it is necessary to consider the main processes occurring when Ln^{3+} compounds exhibit luminescence. In the absence of organic ligand environments, absorption and emission are due to f-f transitions in the electron shells of lanthanides which, at least theoretically, are possible for all ions on going from Ce^{3+} ($4f^{15}d^{1}$) to Yb^{3+} ($4f^{13}$). At the same time, the structure of the levels first becomes progressively more complicated on going from Ce^{3+} to Eu^{3+}, and then gradually becomes simpler on going from Tb^{3+} to Yb^{3+} ion. It is relevant that symmetric ions with respect to Gd^{3+}, located in the center of the Ln series, have some similarity both in the structure of electronic levels and in luminescence features, such as the lifetime of the excited state (**Figure 1**).

The largest energy gap between the excited and ground levels is observed for the Gd^{3+} ion and corresponds to UV emission. Among those emitting in the visible region (**Table 1**), the most efficient phosphors are Tb^{3+} and Eu^{3+} ions; Sm^{3+} and Dy^{3+} ions are

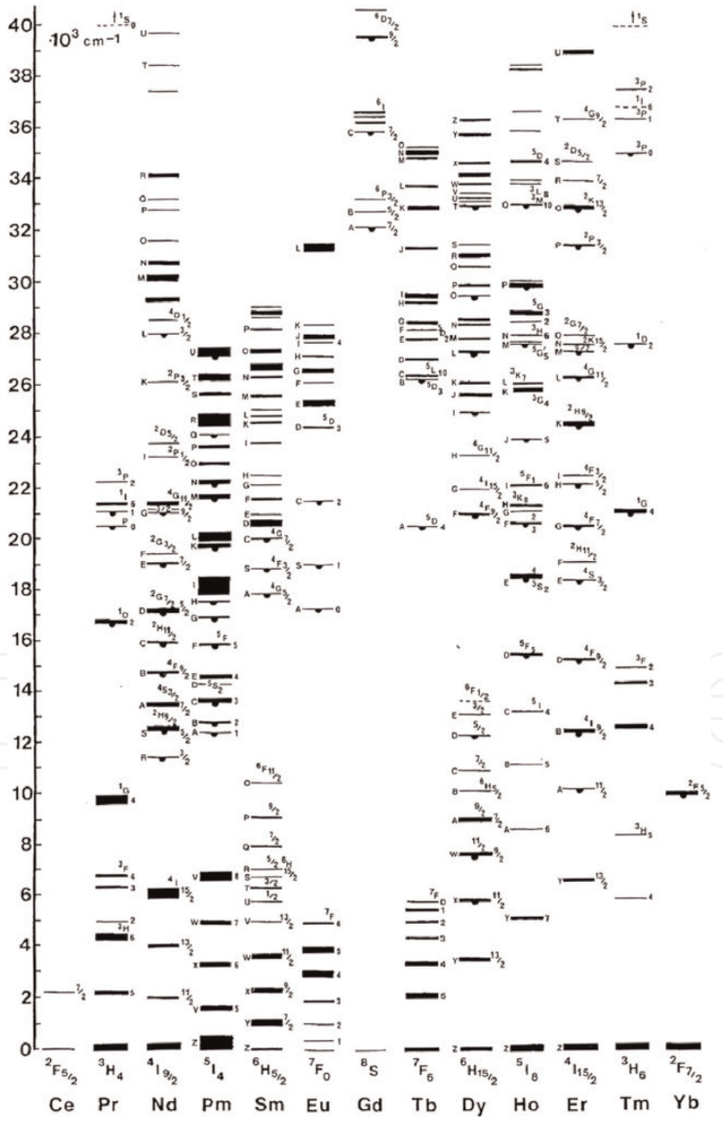

Figure 1.
Free ion energy levels of the trivalent lanthanide ions from Ce^{3+} ($4f^{1}$) to Yb^{3+} ($4f^{13}$). Levels are labeled by term symbols or, for some higher levels, capital letters. Reprinted from Dieke and Crosswhite, 39 copyright 1963, with permission from the Optical Society of America [13].

Ion, electronic configuration	Excited state	Emission ground state	λ_{EM}, nm	Emission color	τ_{H2O}, μs [ref]	τ_{D2O}, μs [ref]
Ce [Xe]$4f^1$	^2D	$^2F_{7/2}$ $^2F_{5/2}$	351 365	UV		
Pr [Xe]$4f^2$	$^3P_0$ (20500) $^1D_2$	^3H_j, j = 4,5,6 $^3F_4$	488, 528, 6,111,050	Red NIR		
Nd[Xe]$4f^3$	$^4F_{3/2}$ (11460)	^4I_j, j = $^9/_2$–$^{13}/_2$ j = $^{15}/_2$–$^9/_2$	900, 1060, 1350	NIR	0.031 [14] 0.031 [15]	0.14 [15]
Sm [Xe]$4f^5$	$^4G_{5/2}$ (17900) $^4G_{5/2}$, $^4G_{5/2}$	^6H_j, j = $^5/_2$–$^{13}/_2$ ^6F_j, j = $^1/_2$–$^9/_2$ $^6H_{13/2}$	560, 595, 640, 700, 775 870, 887, 926, 1010 1150 877	Orange, NIR	2.69 [14] 2.7 [15] 10 $SmCl_3.6H_2O$	60 [15]
Eu [Xe]$4f^6$	$^5D_0$ (17300) $^5D_1$ $^5D_2$	^7F_j, j = 0–6 ^7F_j, j = 0–4 ^7F_j, j = 0–4	580, 590, 615, 650, 720, 750, 820 525, 535, 557, 585, 625 462, 470, 487, 510, 535	Red	112.4 [14] 108 [15]	4020 [14] 4100 [15]
Gd [Xe]$4f^7$	$^6P_{7/2}$ (32200)	$^8S_{7/2}$	315	UV	1480 [14]	
Tb [Xe]$4f^8$	$^5D_4$ (20500)	^7F_j, j = 6–0	490, 545, 580, 620, 650, 660, 675	Green	442 [14] 467 [15]	3800 [15]
Dy [Xe] $4f^9$	$^4F_{9/2}$ (21100) $^4I1_{5/2}$	^6H_j, j = $^{15}/_2$–$^9/_2$ ^6H_j, j = $^{15}/_2$–$^9/_2$	475, 570, 660, 750 455, 540, 615, 695	Yellow- green	2.49 [14] 2.6 [15]	42 [15]
Ho [Xe]$4f^{10}$	$^5F_5$ $^5I_6$ $^5F_4$ (18500)	$^5I_7$ $^5I_8$ ^5I_j, j = 8,7,6	965 1180 540, 750, 1015	NIR NIR Green +NIR		
Er [Xe]$4f^{11}$	$^4S_{3/2}$ $^4F_{9/2}$ ^4I_j, j = 9,11,13 (11750)	$^4I_{15/2}$ $^4I_{15/2}$ $^4I_{15/2}$	550 670 850, 980, 1560	Green Red NIR		
Tm [Xe]$4f^{12}$	$^3H_4$ (12400) $^1G_4$	$^3F_4$ $^3H_6$ $^3H_6$	1470 808 480	NIR NIR Blue		
Yb [Xe]$4f^{13}$	$^2F_{5/2}$ (10250)	$2F_{7/2}$	980	NIR	0.17 [15]	3.95 [15]

[a] *λ_{EM} – emission wavelenght, $\tau_{H2O\ and}$ τ_{D2O} – observed excitation state lifetime of Ln^{3+} solvated with H_2O or D_2O respectively.*

Table 1.
Ions emitting in the visible region.[a]

somewhat lower emitters. Among the IR-emitting ions, the most effective is Yb^{3+}, as well as Nd^{3+} and Er^{3+}. Ce^{3+} luminescence is possible due to d-f electronic transitions. Other ions (Pr^{3+}, Pm^{3+}, Ho^{3+}, Tm^{3+}) can exhibit emission in the visible and/or IR regions, however, as a rule, their intensity is low and difficult to detect with a common equipment. These considerations explain why europium and terbium

compounds are used in most of the productions of lanthanide-based luminescent sensors.

With the exception of the d-f transitions for Ce^{3+} and Tb^{3+}, the electronic transitions of lanthanides are characterized by low extinction coefficients (**Table 2**). The extinction coefficients are significantly lower not only with respect to those found for organic molecules but also with respect to d-cations which cause a low luminescence brightness of most inorganic REE compounds. In 1942, Weissman proposed a solution to this problem [16]. In chelate complexes containing organic ligands characterized by conjugated aromatic fragments, absorption and emission are spatially separated due to the "antenna" effect: the organic molecule effectively absorbs radiation, sequentially passing to singlet and triplet excited states, and then it can transfer

Ion	Transition	Λ	ε, M^{-1} cm^{-1}
Ce^{3+}	$4f^1 \rightarrow 5d$	253	755
	$^2F_{5/2} \rightarrow {}^2F_{7/2}$	~5000	n/d
Pr^{3+}	$^3H_4 \rightarrow {}^3P_2$	444.0	10.1
	$^3H_4 \rightarrow {}^3P_1$	468.8	4.4
	$^3H_4 \rightarrow {}^3P_0$	482.2	4.1
	$^3H_4 \rightarrow {}^1D_2$	589.0	4.95
Nd^{3+}	$^4I_{9/2} \rightarrow {}^4D_{3/2}$	354.0	2.30
	$^4I_{9/2} \rightarrow {}^4G_{9/2}$	512.0	1.89
	$^4I_{9/2} \rightarrow {}^4G_{7/2}$	522.0	3.74
	$^4I_{9/2} \rightarrow {}^4G_{5/2}, {}^2G_{7/2}$	575.2	6.00
	$^4I_{9/2} \rightarrow {}^4S_{3/2}$	731.5	3.80
	$^4I_{9/2} \rightarrow {}^4F_{7/2}$	740.0	6.22
	$^4I_{9/2} \rightarrow {}^4F_{5/2}$	794.0	8.10
	$^4I_{9/2} \rightarrow {}^2H_{9/2}$	801.0	5.48
	$^4I_{9/2} \rightarrow {}^4F_{3/2}$	865.0	3.10
Sm^{3+}	$^6H_{5/2} \rightarrow {}^6P_{3/2}$	401.5	1.25
	$^6H_{5/2} \rightarrow {}^6F_{9/2}$	1089.0	2.19
	$^6H_{5/2} \rightarrow {}^6F_{7/2}$	1250	2.0
Eu^{3+}	$^7F_0 \rightarrow {}^5F_4$	298.0	1.04
	$^7F_0 \rightarrow {}^5H_6$	317.5	0.98
	$^7F_0 \rightarrow {}^5L_6$	396.0	2.90
Gd^{3+}	$^8S_{7/2} \rightarrow {}^6I_{13/2}$	272.7	3.16
	$^8S_{7/2} \rightarrow {}^6I_{11/2}$	273.0	1.12
	$^8S_{7/2} \rightarrow {}^6I_{9/2}, {}^6I_{7/2}$	275.6	1.90
Tb^{3+}	$4f_8 \rightarrow 4f_7{\cdot}5d$	219	374
	$^7F_6 \rightarrow {}^5G_5$	377	n/d
	$^7F_6 \rightarrow {}^5D_3$	385	n/d
	$^7F_6 \rightarrow {}^5D_4$	492	n/d

Ion	Transition	Λ	ε, M^{-1} cm^{-1}
Dy^{3+}	$^6H_{13/2} \rightarrow {}^6P_{3/2}$	325.0	1.88
	$^6H_{13/2} \rightarrow {}^6P_{7/2}$	350.5	2.60
	$^6H_{13/2} \rightarrow {}^4M_{19/2}$	365.0	2.14
	$^6H_{13/2} \rightarrow {}^6F_{5/2}$	807.0	1.84
	$^6H_{13/2} \rightarrow {}^6F_{7/2}$	908.5	2.40
	$^6H_{13/2} \rightarrow {}^6F_{9/2}$, $^6H_{7/2}$	1102.0	1.80
	$^6H_{13/2} \rightarrow {}^6F_{11/2}$, $^6H_{9/2}$	1300.0	1.07
Ho^{3+} Ce^{3+} Tm^{3+} Yb^{3+}	$^5I_8 \rightarrow {}^3F_4$, $^5D_4$	241.0	3.18
	$^5I_8 \rightarrow {}^3H_4$	278.0	2.21
	$^5I_8 \rightarrow {}^3D_4$	287.5	3.10
	$^5I_8 \rightarrow {}^3H_6$	361.5	2.10
	$^5I_8 \rightarrow {}^3G_5$	416.1	2.52
	$^5I_8 \rightarrow {}^3G_6$	452.0	3.70
	$^5I_8 \rightarrow {}^5F_3$	485.5	1.75
	$^5I_8 \rightarrow {}^5F_4$	536.5	4.55
	$^5I_8 \rightarrow {}^5F_5$	641.0	3.04
	$^4I_{15/2} \rightarrow {}^4D_{7/2}$	255.0	6.66
	$^4I_{15/2} \rightarrow {}^4G_{11/2}$	379.2	6.90
	$^4I_{15/2} \rightarrow {}^4F_{7/2}$	487.0	2.03
	$^4I_{15/2} \rightarrow {}^2H_{11/2}$	523.0	3.28
	$^4I_{15/2} \rightarrow {}^4F_{9/2}$	652.5	2.04
	$^3H_6 \rightarrow {}^3P_2$	262.0	1.05
	$^3H_6 \rightarrow {}^3D_2$	360.0	0.93
	$^3H_6 \rightarrow {}^3F_3$	683.0	2.36
	$^3H_6 \rightarrow {}^3H_4$	787.4	1.00
	$^3H_6 \rightarrow {}^3H_5$	1230.0	1.00
	$^2F_{7/2} \rightarrow {}^2F_{5/2}$	973	2.1

Table 2.
Absorption coefficients of Ln^{3+} ions corresponding to the most significant transitions [15].

excitation energy to the Ln^{3+} ion, which in turn emits a typical narrow-band lanthanide-centered emission [17]. In **Figure 2**, a scheme showing the emission mechanism of the luminescence of lanthanide complexes is reported.

It is worth considering the Jabłoński diagram in **Figure 3** to better understand the principles governing luminescence for sensory materials.

Processes occurring during antenna sensitization of lanthanide cations are schematically presented in the Jabłoński diagram (**Figure 3**). Light absorption (A) occurs mainly due to the chromophore groups of the ligand, and the extinction coefficient of the ligand can exceed that of the lanthanide ion by several orders of magnitude [18]. The coordinated ligand is excited to one of the singlet excited states ***S****, the transition

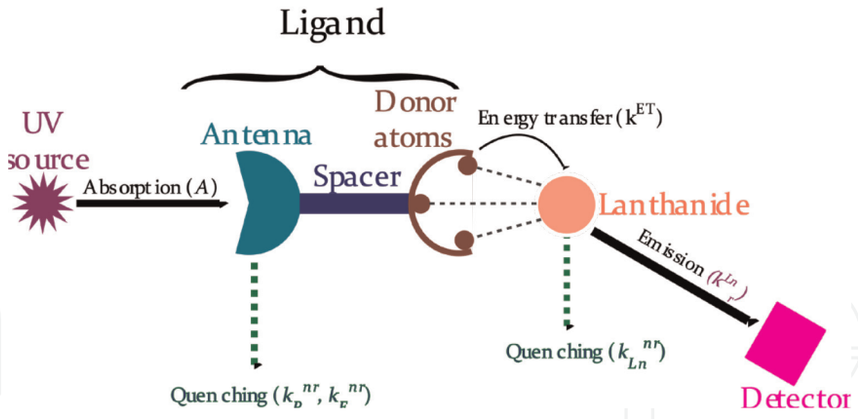

Figure 2.
The emission process for a Ln^{3+} luminescent complex. Antenna, spacer, coordination site, and central ion are evidenced.

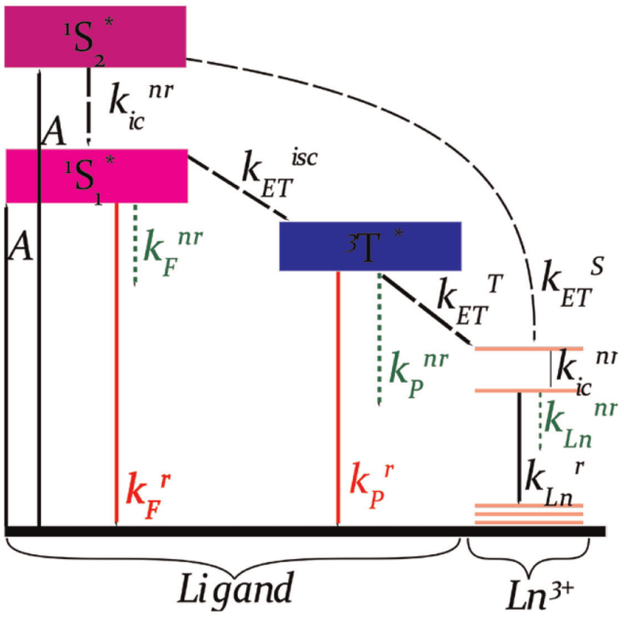

Figure 3.
Simplified Jabłoński diagram for luminescent Ln^{3+} complexes. The processes of absorption (A), radiative relaxation (abbreviated as r) – fluorescence (F), phosphorescence (P), and emission of lanthanides (Ln) are shown by straight lines; nonradiative relaxation processes (nr) are indicated by dotted lines; energy transfer (ET), internal conversion (ic), and intercombination conversion (isc) are indicated by dashed-dotted lines. The reverse energy transfer processes are not shown for clarity.

to the most stable state being defined as internal conversion (k_{ic}^{nr}). At this stage, the ligand can either emit a quantum of light (ligand fluorescence, rate constant k_F^r), or non-radiatively relax (k_F^{nr}), or its excited state S^* energy can be transferred to the triplet excited state $^3T^*$ by inter-combination conversion (k_{isc}). This triplet state is relatively long-lived due to the forbiddance of singlet-triplet transitions. The luminescent relaxation of the triplet excited state is called phosphorescence (k_P^r) and is well observed when the energy of $^3T^*$ is lower than the resonant level of lanthanide. This is usually the most common phenomenon for Gd^{3+} complexes [19]. The triplet excited state life is longer than that of the singlet one. Various relaxation pathways are possible for it: ligand phosphorescence (k_P^r), nonradiative relaxation (k_P^{nr}) due to energy transfer into lattice vibrations (multiphonon relaxation), and energy transfer to the lanthanide ion (k^T_{ET}). In addition to this pathway, in rare cases, direct

excitation of the lanthanide ion through the singlet state of the ligand ($k_{ET}{}^{S}$) is also recorded. The transitions inside the f-shells of lanthanides are quite fast and are accompanied by the luminescence of the latters ($k_{Ln}{}^{r}$). Nonradiative relaxation of the excited states of lanthanides due to phonon lattice vibrations is also possible, which corresponds to the constant $k_{Ln}{}^{nr}$.

Thus, the luminescence efficiency of monometallic lanthanide complexes depends on the rate of many processes, and minor changes in the system can dramatically affect it. To date, some rules have been developed that are necessary for the production of efficient luminescent materials based on REE compounds, primarily Eu^{3+} and Tb^{3+}, but also Sm^{3+}, Dy^{3+}, IR-emitting Nd^{3+}, Yb^{3+}, and some other REE ions [17, 19–21].

3. Classification of sensory materials

There are several ways to classify sensory materials:

i. according to the type of response;

ii. according to the structural features;

iii. according to the Ln^{3+} ions employed;

iv. according to the mechanisms leading to the occurrence of the response.

In this manuscript we will consider examples of various materials, classifying them according to the type of recorded response, and evidencing also other relevant features.

From a phenomenological point of view, the most rational classification is on the basis of the type of *sensory signal being recorded*, the most common being "turn on", "turn off" and "ratiometric". These types of sensory response are unevenly represented in the literature (**Figure 4**). The most common type of response, i.e. the "turn off", is characterized by the least selectivity and unfortunately is not optimal for practical use.

It makes sense to distinguish the materials according to their structural features and typology. For example, it is useful to differentiate between soluble mononuclear

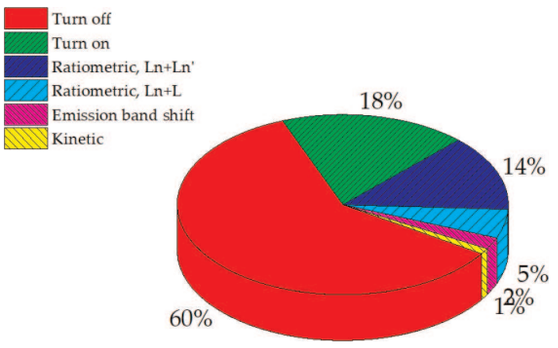

Figure 4.
Percentage of different types of sensory response in lanthanide-based luminescent sensors.

complexes, coordination polymers (CP's) and porous Metal–Organic Frameworks (MOF's) [22], or immobilized species on an inorganic support surface. Each of these materials has both advantages and disadvantages, and it is impossible to unambiguously define them as optimal without specifying the conditions for which they are optimal. For example, molecular complexes quickly react with an analyte and are convenient objects for studying the response mechanism; however, their regeneration is complicated, and they contaminate the sample. Complexes immobilized on carriers react more slowly and their preparation is time-consuming. Synthesis of insoluble MOF's is often even more difficult, but they offer the advantages of high chemical stability and increased selectivity due to limited pore and channel permeability.

A third possible classification of materials is according to the type of luminescent centers used:

a. materials that contain cations that effectively give luminescence, for example, Tb^{3+} or Eu^{3+};

b. materials that contain less intense emitters, for example, Sm^{3+} or Dy^{3+};

c. species containing lanthanide ions often emitting in the IR region (Nd^{3+}, Er^{3+}, Yb^{3+});

d. materials where the luminescence is exclusively due to the ligand;

e. bi- and polymetallic systems with several luminescent centers.

The luminescence efficiency of Eu^{3+} and Tb^{3+} compounds usually turn out to be much higher, moreover, their emission bands lie in the visible region (**Table 1**), where the sensitivity of standard photomultipliers is high. As a result, most of the described sensor materials are built by using Eu^{3+} and Tb^{3+} compounds for "turn on", "turn off", and "ratiometric" sensors. The luminescence of IR-emitting ions Nd^{3+}, Er^{3+}, and Yb^{3+} are more sensitive to C–H bond vibrations, which makes them also promising to produce special sensor materials.

Finally, the fourth classification method allows one to distinguish between materials according to the mechanism of sensory response. The proposed classification is based on the effect that the analyte has on both the structure of the complex and on the processes reflected in the Jabłoński diagram.

The most obvious is the mechanism of action defined "**internal filter**"**effect** (**IFE**), in which the absorption spectrum of the analyte overlaps with the excitation or luminescence band of the sensor material. This mechanism (**Figure 5**) is not characterized by high selectivity and sensitivity but can be easily implemented for many analytes, for example, Fe^{3+} ions. For obvious reasons, only a "turn off" response can be achieved for materials based on this principle. The IFE does not require chemical interaction of the analyte with the sensor material. The unequivocal evidence of the involvement of the IFE mechanism in the sensory response is the intersection of the spectra.

The second, also relatively simple, response mechanism involves either the coordination of the antenna molecule to the lanthanide complex or the elimination of the antenna molecule and its replacement with a non-antenna analyte molecule. In the first case, a turn on response is observed, and in the second, a turn off. Proof for this

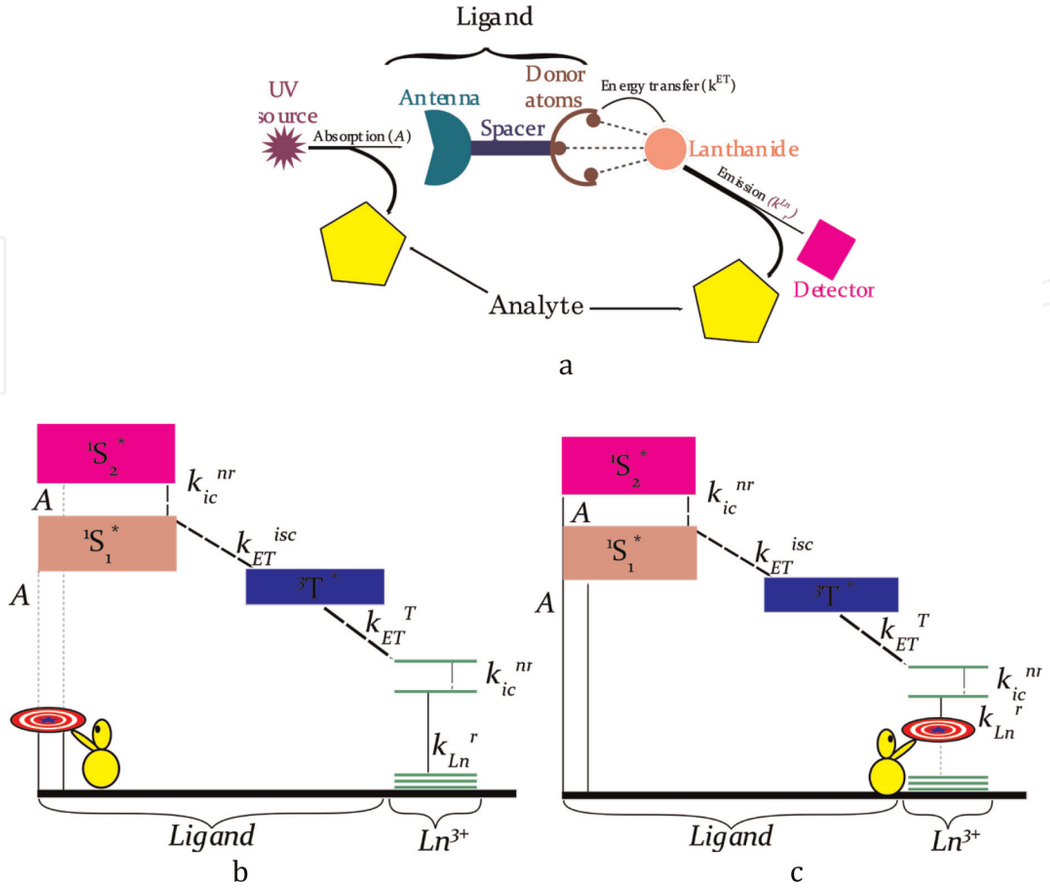

Figure 5.
Response mechanism associated with the internal filter effect: a) - the effect of the analyte on the luminescence of the sensor molecule; b) Jabłoński diagram when the analyte absorbs excitation energy; c) Jabłoński diagram for the absorption of the radiation emitted by the analyte.

mechanism can derive from analytical and spectroscopical data confirming the change in the structure of the complex.

The third possible mechanism, **analyte switching antenna** (**ANA**) is associated with a change in the structure of the ligand, "turning on" or "turning off" the antenna function (**Figure 6a**). In this case, the analyte changes either the absorption efficiency of the ligand (A) (**Figure 6b**), or the energy of the singlet and triplet levels (***S****, ***T****) (**Figure 6c**), or the sensitization efficiency (k^T_{ET}) (**Figure 6d**), but the analyte itself should not have absorption in the region of excitation or emission of the sensor and should not have a direct effect (antenna sensitization or quenching) on the Ln^{3+} ion, otherwise other possible mechanisms (effect of an internal filter, energy transfer, vibrational quenching of luminescence) take place in parallel with this mechanism or dominate it. In a typical case related to this mechanism, the sensor molecule contains an antenna group, a macrocyclic analyte receptor as a spacer, and a lanthanide ion in a suitable environment. The coordination of M^{n+} by a macrocyclic receptor leads to a change in the electronic structure of the ligand, although the cation itself (usually an alkali or alkaline earth metal) does not affect the luminescence of other Ln^{3+} compounds.

Depending on the nature of the substance, both "turn off" and "turn on" responses can be realized. It is not easy to prove the existence of an ANA mechanism; it is necessary to show the formation of a ligand-analyte bond by analytical methods and to detect a change in the efficiency of specific processes using spectroscopic, kinetic, and/or calculation methods.

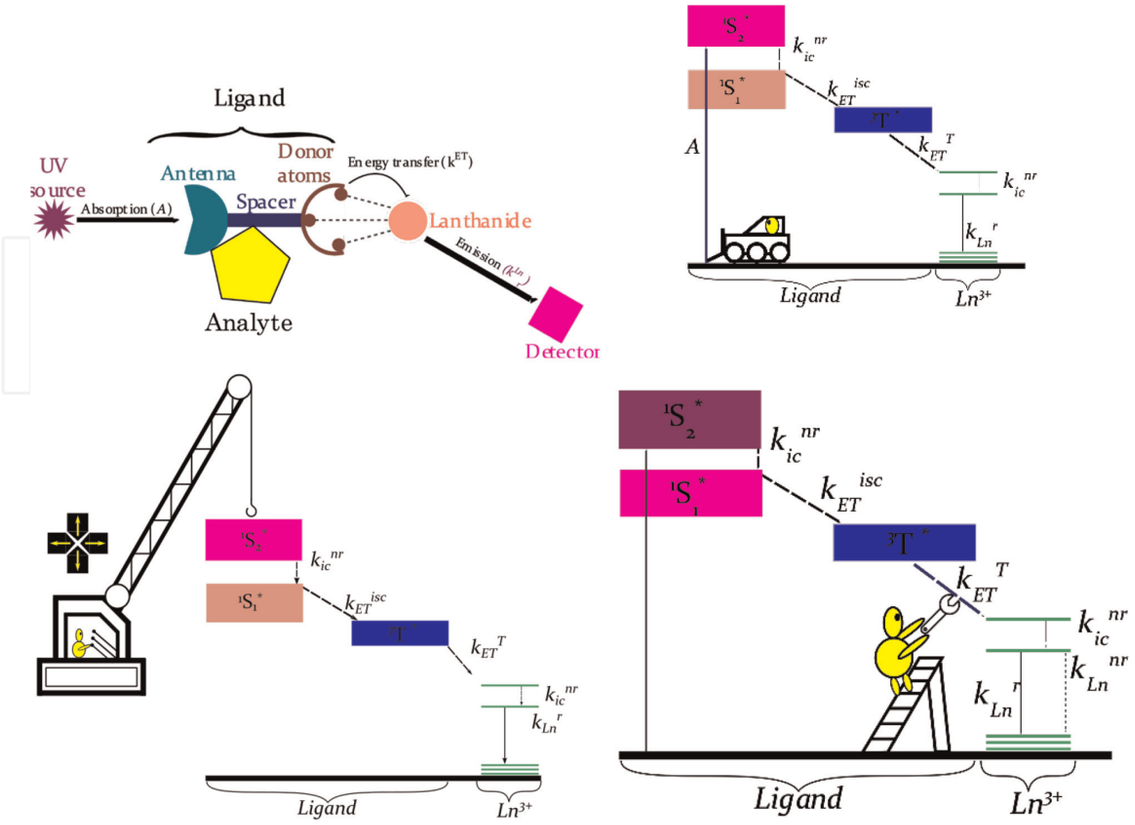

Figure 6.
Response mechanisms associated with an analyte-switched antenna (ANA). An analyte with its o antenna function is inserted into the structure of the complex (a). As a result, we have a change in the absorption efficiency (b), of the energy of the singlet or triplet level (c), and finally of the sensitization efficiency (d).

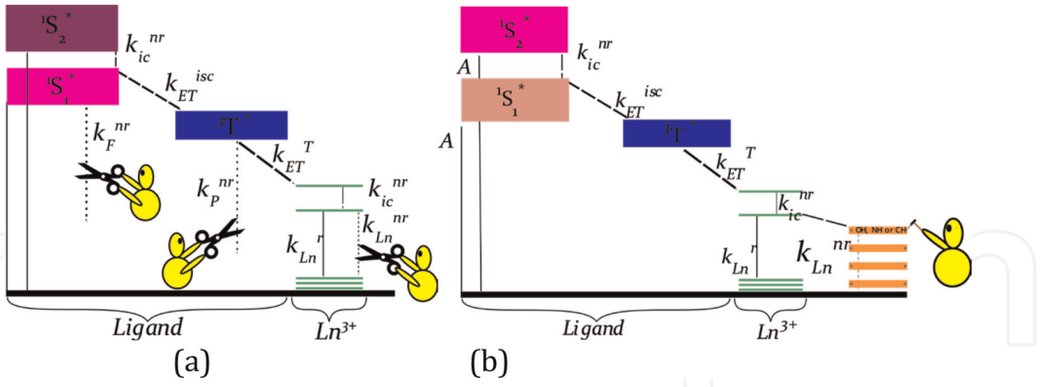

Figure 7.
Response mechanisms associated with the control of luminescence quenching processes (quencher addition/elimination, QAE). Suppression of nonradiative relaxation of the singlet, triplet states, and the excited state of lanthanide (a). Controlling vibrational quenching by introducing or removing X-H bonds (b).

The fourth possible mechanism is the addition or elimination (due to oxidation, substitution, or another process) of the quencher group during the interaction of the sensor with the analyte (quencher addition/elimination, QAE mechanism) (**Figure 7**). Bonds with suitable vibrational energy (OH, NH, CH) can act as quenching groups: in fact, the excited state of Ln^{3+} or the ligand upon interaction with the analyte can effectively undergo phonon relaxation. This mechanism involves the transformation of the sensor molecule into a new compound, which can be confirmed by analytical

chemistry and spectroscopy. A "turn off" or a "turn on" response is observed depending on whether the groups are attached or split off. When a quenching group (for example, H_2O) is replaced by an antenna ligand, two possible processes simultaneously contribute: removal of the quencher and enhancement of sensitization by the new antenna molecule or the reverse process.

The fifth possible mechanism can be observed when the sensor material is a bimetallic system containing two lanthanum ions, usually Tb^{3+} and Eu^{3+}. Due to the proximity of radii and chemical properties, in these compounds, the two cations, as a rule, occupy the same crystallographic positions and are statistically distributed. If both Ln^{3+} ions are capable of emission, the excitation energy is transferred between the ions, and the rate constant of this process can be determined from kinetic data [23]. If the analyte affects the energy transfer constant between the ions, then a sensory response appears, which manifests itself as a change in the ratio of the integral luminescence intensities of the lanthanum ions. The proof of this mechanism requires a careful analysis of spectroscopic and kinetic data and cannot be extended to any "ratiometric" sensors, since in many cases, at least in the case of detection of CH, OH, and NH bonds, the response is not associated to a change in the efficiency of sensitization of one lanthanide ion by another, but with more efficient quenching of the luminescence of one of the ions.

Finally, also materials that are potentially usable as thermometric sensors can be based on REE compounds. However, the discussion on this topic is beyond the scope of this review. Lanthanide-containing luminescent thermometers are the subject of special reviews and monographs [24, 25].

The internal nature of the f-shells of lanthanides makes them less susceptible to the effects of the crystal field, however, a change in the geometry of the coordination environment can still be detected in several cases by careful analysis of the luminescence spectra. This principle is applicable in gauge sensors, in which compression of the crystal under pressure leads to a reduction in the Ln-O [26, 27] or Ln-F [28, 29] distances, which shifts the bands in the emission spectrum.

4. Turn off sensors

Recent papers describing luminescent sensor materials have reported clearly that "turn off sensors" dominate other types of response. This can be easily explained by the fact that luminescence quenching due to IFE, nonradiative relaxation of the excited states of the complex, or formation of a not-luminescent complex (static quenching) are caused by a large number of analytes with a different chemical nature [30]. Turn off sensors are poorly usable in real devices since it is difficult to detect signals at a low analyte concentration.

Effective internal filters can be either intensely colored compounds (due to d-d transitions typical of d-cations as Cu^{2+} or Co^{2+}, or to charge-transfer bands as in hydrolyzed Fe^{3+} aqua ions, $Cr_2O_7^{2-}$, CrO_4^{2-}, MnO_4^- anions).

The nonradiative relaxation of the excited state of the complex obeys the Stern-Volmer equation:

$$\frac{I_0}{I} = \frac{PLQY_0}{PLQY} = \frac{\tau_0}{\tau} = 1 + K_{SV}^D[Q]$$

where K^D_{SV} – is the dynamic Stern-Volmer constant [31]. The higher the K^D_{SV} value, the higher the sensitivity of the sensor material with respect to the quenching analyte. In the case of dynamic quenching, in addition to the luminescence intensity (and quantum yield), the lifetime of the excited state of Ln^{3+} is significantly reduced. Dynamic quenching is caused by the excitation energy adsorption from the quencher molecule without the formation of a phosphor-quencher bond.

Static quenching is caused by the formation of a non-luminescent complex formed by the luminophore and quencher molecules. The bond between the two species can be either covalent or hydrogen or stacking interaction. Static quenching is associated with nonradiative deactivation of the singlet or triplet state of the ligand, which weakens the antenna sensitization. As a result, during static quenching, the observed lifetime of the excited state (τ_{obs}) of the lanthanide ion can slightly decrease, but to a lesser extent with respect to the dynamic quenching. For static quenching, the Stern-Volmer equation is also applicable:

$$\frac{I_0}{I} = 1 + K^S_{SV}[Q]$$

In many cases, these two types of quenching complement each other, and by combining the equations for the static and dynamic cases the following generalized equation can be derived:

$$\frac{I_0}{I} = 1 + \left(K^D_{SV} + K^S_{SV}\right)Q + K^D_{SV} \times K^S_{SV} \times Q^2$$

The nonlinear dependence of I_0/I on the quencher concentration Q indicates a complex quenching mechanism.

Measurements carried out with a temperature control also make it possible to distinguish between static and dynamic quenching mechanisms, since for a static mechanism, an increase in temperature leads to a decrease in K_{SV} and for a dynamic one, to an increase [31].

The luminescence quenching can occur via excitation energy transfer (ET) from the ligand or metal through FRET (Förster Resonance Energy Transfer), DEE (Dexter Electron Exchange), or PET (Photoinduced Electron Transfer) mechanisms [32] (**Figure 8**) which imply the deactivation of the excited state of the molecule by transferring the excitation energy to the quencher molecule, whose LUMO is lower in energy with respect to the excited electron of the donor molecule.

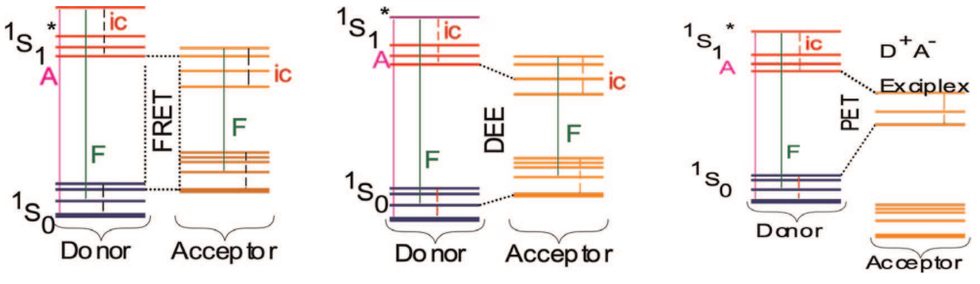

Figure 8.
Schematic representation of the mechanisms of deactivation of excited states. Left - Förster mechanism (FRET), center – Dexter mechanism (DEE), right – photoinduced electron transfer (PET) mechanism.

FRET [33] implies nonradiative energy transfer from an excited donor molecule to an unexcited acceptor molecule, followed by radiative or nonradiative relaxation of the latter. The typical distances between the donor and acceptor molecules usually are 20–60 Å, and the efficiency of the Förster transfer decreases very rapidly with increasing distance (efficiency is proportional to r^{-6}), which makes it possible to measure the distance between particles. A transfer is described as the emission and absorption of a virtual photon [34].

DEE [35] includes two electronic transitions: an excited electron from the donor molecule to the LUMO of the acceptor molecule, and an electron from the HOMO of the donor to the HOMO of the acceptor. This creates a hole in the HOMO of the donor molecule [36]. These two processes proceed either simultaneously or sequentially. This mechanism is observed at much shorter distances (less than 10 Å) and is associated with the need for direct overlapping of the wave functions of the fluorophore and quencher. The efficiency of DEE quenching also decreases very rapidly with increasing distance (proportional to e^{-r}).

Another common mechanism of nonradiative relaxation of an excited state is PET [37] involving the formation of a charge-transfer complex (exciplex). An exciplex is formed when an electron moves from a LUMO donor to a LUMO acceptor, followed by radiative or nonradiative relaxation of the latter. An increase in the distance between the donor and acceptor has a much smaller effect on the efficiency of PET quenching with respect to FRET and DEE mechanisms.

To distinguish between these mechanisms, special quantum chemical methods are used to determine the HOMO and LUMO energies, as well as the dependence of the quenching efficiency on the distance between the donor and acceptor. Often, the real quenching mechanism has not been studied in detail, the PET or FRET quenching being only postulated.

The most common analytes detected with lanthanide-containing "turn off" sensors are listed in **Table 3**. Data on the mechanisms of sensory response are not always reported, moreover, in some cases, the author's interpretation of the mechanism may not be entirely correct. In several cases a static quenching mechanism associated with analyte-sensor bonds due to hydrogen bonds, stacking, and other weak interactions is suggested. Unfortunately, in most works, a more detailed mechanism of such static quenching has not been reported.

Analyte	**Mechanism**	**Ref.**
i. id-metal cations		
Cr^{2+}	Static quenching	[38]
Cr^{3+}	ET, IFE	[39, 40]
Mn^{2+}	Shift of the triplet level of the ligand during the coordination of the analyte	[41]
Fe^{2+}	Static quenching	[42]
Fe^{3+}	IFE, ET, Static quenching	[43–87]
Co^{2+}	ET, IFE, Static quenching	[88, 89]
Ni^{2+}	IFE, LMET	[90]
Cu^{2+}	IFE, LMET	[63, 69, 88, 91–99]
Ag^{+}	Shift of the triplet level of the ligand during the coordination of the analyte	[41, 66]

Analyte	Mechanism	Ref.
Hg^{2+}	IFE [100], Shift of the triplet level of the ligand during the coordination of the analyte, Static quenching [101, 102]	[100–102]
ii. p-metal cations		
Pb^{2+}	Shift of the triplet level of the ligand during the coordination of the analyte Static quenching [102, 103]	[102–104]
Al^{3+}	n/a,	[105, 106]
Ce^{3+}	IFE, Static quenching	[74]
UO_2^{2+}	n/a	[87]
iii. d-metal anions		
MnO_4^-	IFE, FRET	[106–108]
CrO_4^{2-}, $Cr_2O_7^{2-}$	IFE, FRET	[55, 77, 94, 105, 107–112]
ClO^-	Destruction of the ligand, weakening the antenna function	[113]
F^-	Displacement of the ligand by the analyte	[114]
HSO_4^-	Static quenching due to the H-bonding	[115]
$H_2PO_4^-$	Static quenching due to the H-bonding	[115]
CN^-	Static quenching due to the H-bonding. Possible destruction of the complex due to the binding of Zn^{2+} ions by CN^-	[116]
OAc^-	Static quenching due to the H-bonding	[116]
iv. Other organic analytes		
Nitroaromatic compounds	PET and IFE	[44, 46, 47, 67–71, 73, 75, 76, 85, 90, 94, 97, 99, 117–130]
Nitromethane	IFE	[53, 73]
$PhNH_2$	Static quenching due to the H-bonding и IFE	[131]
PhCHO	Static quenching due to the H-bonding	[40, 50, 132–134]
Chlorobenzenes	IFE	[135]
Acetone	Static quenching due to the H-bonding	[52, 54, 91, 99]
DMAA	n/a	[136]
Tryptophan	n/a	[59]
Tiaminphosphate derivatives	ET	[137, 138]
Acetophenone	n/a, but not the IFE	[139]
1-hydroxypyrene	Static quenching due to the H-bonding	[140]
Pesticides	Static quenching, IFE, FRET	[141]
Sulfamethazine	IFE	[142]
Ornidazole, Ronidazole	IFE&Energy transfer	[66]
Adenosine diphosphate	Static quenching	[115]

Analyte	Mechanism	Ref.
Quercetin	IFE	[62]
Nitrofuranose, Nitrofurantoin	PET IFE	[143]
Phenylglyoxylic acid	IFE	[144]

Table 3.
Proposed sensory response mechanism in turn off sensors employed to detect different analytes.

It should be noted that the most common mechanism is IFE. Typical excitation spectra of luminescent lanthanide complexes lie in the near UV region in the range 250–400 nm [4, 6, 145]. In this region, intense absorption of several types of analytes takes place, which makes such materials nonselective, although the selectivity has not been investigated in most of the articles.

The most efficient materials for the detection of various analytes are listed in **Table 4**. Materials with high K_{sv} values (>30,000) are selected as illustrative examples, making these materials potentially promising for practical applications.

Material	Media	Linearity range	K_{SV}. M^{-1}	LOD	Response time	Ref.
Fe^{3+} sensors						
Tb-MOF	DMF	0–100 μM	43,000	0.5 μM		[73]
Eu-MOF	DMF	0–140 μM	51,600	0.5 μM		[73]
Tb-MOF	EtOH	0.01–100 μM	114,300			[64]
Eu-MOF	EtOH	0–10 mM	43,000	1 μM	8 min	[63]
Tb-MOF	H_2O		65,000	0.84 μM		[57]
Tb-MOF	H_2O	0–1 mM	96,021		24 h	
Eu-MOF	H_2O	0–1 mM	75,596		24 h	[52]
Eu-MOF	H_2O	5–12 μM	119,000	0.277 μM		[66]
Cu^{2+} sensors						
Nd-MOF	CH_3CN	0–100 μM	80,000	0.39 μM		[88]
Eu-MOF	EtOH	0–10 mM	52,000	1 μM	8 min	[63]
Cr^{2+} sensors						
Eu-MOF	H_2O	0–100 μM	39,000			[38]
Tb-MOF	H_2O	0–100 μM	50,000			[38]
Co^{2+} sensor						
Nd-MOF	CH_3CN	0–60 μM	66,000	0.47 μM		[88]
Ag^{+} sensor						
Eu-MOF	H_2O	10–19 μM	118,000	0.272 μM		[66]
Pb^{2+} sensor						

Material	Media	Linearity range	K_{SV}. M^{-1}	LOD	Response time	Ref.
Eu-MOF	H_2O DMF	10–500 μM	33,014 43,988	91 μM 68 μM		[102]
$Cr_2O_7^{2-}$ sensors						
POSS-PVIM@[Eu(dbm)$_3$] hybrid material	H_2O	5–40 μM	42,014	0.68 μM	5 min	[111]
[Eu-MOF	H_2O	0–200 μM	220,000		6 min	[55]
Tb-MOF	H_2O	0–100 μM	41,100	5.6 ppb	5 min	[112]
Tb-MOF	H_2O	0–3 μM	106,500	0.32 μM		[77]
Eu-MOF	H_2O	0–1.5 μM	151,000	0.10 μM		[77]
CrO_4^{2-} sensors						
Tb-MOF	H_2O	0–3 μM	127,500	0.33 μM		[77]
Eu-MOF	H_2O	0–2 μM	102,500	0.17 μM		[77]
TNP sensors						
La-MOF	H_2O	0–20 nM	2.4*109	0.22 ppb		[129]
Nd-MOF	H_2O	0–20 nM	1*107	0.71 ppb		
Pr-MOF	H_2O	0–20 nM	6.8*109	0.27 ppb		
Eu-MOF	DMAA	0–25 μM	49,000	0.34 μM		[130]
Tb-MOF	DMF	0–22 μM	155,000	30 nM	30 min	[71]
Tb-MOF	H_2O	0–40 μM	54,800	0.35 ppm		[118]
Nitrobenzene sensors						
Tb-MOF	H_2O	5–30 ppm	93,400	2.1 ppm		[99]
	H_2O	5–30 ppm	80,300	2.2 ppm		[99]
Eu-MOF	DMF	0–1.6 mM	62,400	5 μM		[119]
$PhNH_2$ sensor						
Eu$(NO_3)_3$Zn-MOF	DMF	0–1 μM	9,390,000	6.6 nM	30 min	[110]
PhCHO sensors						
Tb$(NO_3)_3$ + Zn-MOF	DMF	0–0.2 μM	6,170,000	10 nM	30 min	[110]
Tb-MOF	EtOH	0–0.5%	31,100			[133]
Tb-MOF	EtOH	0–20 μM	33,500	7.71e^{-7} M	30 min	[134]
Yb-MOF	EtOH	0–20 μM	29,900	8.64e^{-7} M	30 min	[134]
Acetone sensor						
Eu-MOF	DMF	5–30 ppm	78,900	10.1 ppm		[99]
Tiamine phosphates chlorides						
Eu-MOF			Up to 900,800	Up to 0.029 μM		[137]
Tb-MOF			Up to 39,000	Up to 0.025 μM		[138]
Sulfamethazine sensor						

Material	Media	Linearity range	K_{SV}. M^{-1}	LOD	Response time	Ref.
Eu-MOF	EtOH-H_2O	0–100 μM	45,980	0.66 μM		[142]
Ornidazole sensor						
Eu-MOF	H_2O	6–18 μM	197,000	0.183 μM		[66]
Ronidazole sensor						
Eu-MOF	H_2O	6–18 μM	212,000	0. 141 μM		[66]

Table 4.
The most sensitive "turn off" touch materials.

The detection of Fe^{3+}, d-metal ions and also d-metal-containing anions with strong oxidizing abilities can be performed by simpler methods with respect to the production of the luminescent sensors. At the same time, the determination of impurities of toxic metals (lead, mercury) in waters or foods seems to be a much more urgent task, and there is hope that other results on the determination of such analytes will appear soon. Nitroaromatic compounds are found in a large number of explosives and ammunition, and proposed sensor materials often exhibit very high sensitivity to them. At present, there are some commercial luminescent "turn off" detectors of nitroaromatic compounds, and although trade secrets prevent disclosure of the compositions of specific materials, lanthanide-containing complexes seem to be promising in this direction. As for the detection of other organic molecules, due to the prevalence of absorption in the near UV region, the industrial production of these materials requires increased selectivity.

Based on the analysis of literature data, we can propose the following algorithm for establishing the sensory response mechanism for "turn off" sensors:

i. A plot of Stern-Volmer graphs at different temperatures to establish the presence of dynamic or static quenching or their simultaneous presence. An exclusively static quenching mechanism indicates the formation of a not-luminescent complex, which, however, requires additional evidence.

ii. A chemical and/or phase analysis of the "sensor-analyte" system, is absolutely necessary to verify the formation of a not-luminescent complex and the destruction of the sensor structure.

iii. A sensory experiment in a deuterated solvent medium to determine if the material is sensitive to water, alcohol, and other molecules with an active OH group. The disappearance of the response unambiguously indicates that OH quenching is the dominant mechanism.

iv. A study of the absorption spectra of the analyte and the excitation spectra of the sensor material. An overlap suggests at least partial involvement of the IFE mechanism. Measurements of the sensory response should be made when the material is excited at a wavelength that does not fall within the absorption spectrum of the sensor, for example, directly at the f-f wavelength of the Ln^{3+} transition. If the response completely disappears, then only the IFE mechanism is in place.

v. A study of the luminescence spectra of the complex and absorption spectra of the analyte. The presence of overlap indicates the partial participation of the IFE mechanism and the possibility of energy transfer through the FRET mechanism.

vi. A quantum-chemical modeling study to determine the energy of orbitals, measurement of τ upon excitation through the bands of the ligand and of metal in the absence and presence of quenchers. In this way, the presence of energy transfer can be confirmed and the specific mechanism (PET, FRET, DEE) can be determined.

5. Conclusions

The luminescence of lanthanide coordination compounds is an unusual and multi-stage process that imposes numerous restrictions on the structure of both ligands and complex compounds. Interruption of any of the intermediate stages due to the *effect of an internal filter*, *nonradiative deactivation* of the excited states of the ligand and metal, *changes in the energy of the triplet level* of the ligand, or other factors dramatically affect the luminescence brightness. This presents a serious challenge in the development of efficient luminescent materials for light-emitting devices, but it can be an elegant key for the development of sensitive sensor materials for the detection of analytes of various natures.

The main problem with *turn off* materials is *low selectivity*, since dissimilar analytes such as nitroaromatic compounds and Fe^{3+} cations, for example, cause exactly the same response. Now, a new challenge for researchers is to find the way to increase the selectivity of the response, which requires the use of modern approaches of supramolecular chemistry and crystal chemical engineering.

In the following chapter, we will focus on consideration of two less common, but more technologically advanced and promising areas in lanthanide-based luminescent chemical sensors – *turn on* and *ratiometric* materials.

Acknowledgements

University of Camerino is gratefully acknowledged.

Conflict of interest

The authors declare no conflict of interest.

DOI: http://dx.doi.org/10.5772/intechopen.109011

Author details

Claudio Pettinari[1*], Andrei Drozdov[2] and Yuriy Belousov[2]

1 School of Pharmacy, University of Camerino, Camerino, Italy

2 Moscow State University, Moscow, Russia

*Address all correspondence to: claudio.pettinari@unicam.it

References

[1] Feng J, Zhang H. Hybrid materials based on lanthanide organic complexes: A review. Chemical Society Reviews. 2013;**42**:387-410. DOI: 10.1039/c2cs35069f

[2] Sun T, Gao Y, Du Y, Zhou L, Chen X. Recent advances in developing lanthanide metal–organic frameworks for ratiometric fluorescent sensing. Frontiers in Chemistry. 2021;**8**. DOI: 10.3389/fchem.2020.624592. Available from: https://www.frontiersin.org/articles/10.3389/fchem.2020.624592

[3] Bünzli JCG, Piguet C. Lanthanide-containing molecular and supramolecular polymetallic functional assemblies. Chemical Reviews. 2002;**102**: 1897-1928. DOI: 10.1021/cr010299j

[4] Bünzli JCG, Piguet C. Taking advantage of luminescent lanthanide ions. Chemical Society Reviews. 2005; **34**:1048-1077. DOI: 10.1039/b406082m

[5] Eliseeva SV, Bünzli JCG. Lanthanide luminescence for functional materials and bio-sciences. Chemical Society Reviews. 2010;**39**:189-227. DOI: 10.1039/b905604c

[6] Eliseeva SV, Bünzli JCG. Rare earths: Jewels for functional materials of the future. New Journal of Chemistry. 2011; **35**:1165-1176. DOI: 10.1039/c0nj00969e

[7] Lee SY, Lin M, Lee A, Park YII. Lanthanide-Doped Nanoparticles for Diagnostic Sensing. Nanomaterials. 2017;**7**:411. DOI: 10.3390/nano7120411

[8] Aulsebrook ML, Graham B, Grace MR, Tuck KL. Lanthanide complexes for luminescence-based sensing of low molecular weight analytes. Coordination Chemistry Reviews. 2018;**375**:191-220

[9] Aletti AB, Gillen DM, Gunnlaugsson T. Luminescent/colorimetric probes and (chemo-) sensors for detecting anions based on transition and lanthanide ion receptor/binding complexes. Coordination Chemistry Reviews. 2018;**354**:98-120

[10] Xu H, Cao CS, Kang XM, Zhao B. Lanthanide-based metal-organic frameworks as luminescent probes. Dalton Transactions. 2016;**45**:18003-18017. DOI: 10.1039/C6DT02213H

[11] Zhao SN, Wang G, Poelman D, Voort PV. Luminescent Lanthanide MOFs: A Unique Platform for Chemical Sensing. Materials. Basel, Switzerland. 2018;**11**(4): 572. DOI: 10.3390/ma11040572

[12] Lunev AM, Belousov YA. Luminescent sensor materials based on rare-earth element complexes for detecting cations, anions, and small molecules. Russian Chemical Bulletin. 2022;**71**:825-857. DOI: 10.1007/s11172-022-3485-3

[13] Van Der Ende BM, Aarts L, Meijerink A. Lanthanide ions as spectral converters for solar cells. Physical Chemistry Chemical Physics. 2009;**11**: 11081-11095. DOI: 10.1039/b913877c

[14] Lis S, Kimura T, Yoshida Z. Luminescence lifetime of lanthanide(III) ions in aqueous solution containing azide ion. Journal of Alloys and Compounds. 2001;**323–324**:125-127. DOI: 10.1016/S0925-8388(01)00980-X

[15] Poluektov NS, Kononeko LI, Efrushina NP, Beltukova SV. In: Pilipenko AT, editor. Spectrophotometric and luminescent methods for the determination of lanthanides. Kiev, USSR: Naukova Dumka; 1989;**256**

[16] Weissman SI. Intramolecular energy transfer the fluorescence of complexes of europium. The Journal of Chemical Physics. 1942;**10**:214-217. DOI: 10.1063/1.1723709

[17] Sato S, Wada M. Relations between intramolecular energy transfer efficiencies and triplet state energies in rare earth β-Diketone chelates. Bulletin of the Chemical Society of Japan. 1970; **43**:1955-1962

[18] Bünzli, J.-C.G.; Eliseeva, S. V. Basics of lanthanide photophysics. 2010; pp. 1–45

[19] Latva M, Takalob H, Mukkala VM, Matachescu C, Rodríguez-Ubis JC, Kankare J. Correlation between the lowest triplet state energy level of the ligand and lanthanide(III) luminescence quantum yield. Journal of Luminescence. 1997;**75**:149-169. DOI: 10.1016/S0022-2313(97)00113-0

[20] Bünzli JCG. Lanthanide luminescence: From a mystery to rationalization, understanding, and applications. Handbook on the Physics and Chemistry of Rare Earths. 2016;**50**: 141-176. DOI: 10.1016/bs.hpcre.2016.08.003

[21] Bünzli J, Eliseeva SV. Basics of lanthanides photophysics. In: Hänninen P, Lanthan HH, editors. Lanthanide Luminescence. Vol. 7. Lumin. Springer Ser. Fluoresc; 2010. pp. 1-45. DOI: 10.1007/4243

[22] Hu Z, Deibert BJ, Li J. Luminescent metal-organic frameworks for chemical sensing and explosive detection. Chemical Society Reviews. 2014;**43**: 5815-5840

[23] Gontcharenko VE, Kiskin MA, Dolzhenko VD, Korshunov VM, Taydakov IV, Belousov YA. Mono- and mixed metal complexes of Eu^{3+}, Gd^{3+}, and Tb^{3+} with a diketone, bearing pyrazole moiety and chf_2-group: Structure, color tuning, and kinetics of energy transfer between lanthanide ions. Molecules. 2021;**26**:1-16. DOI: 10.3390/molecules26092655

[24] Brites CDS, Millán A, Carlos LD. Lanthanides in luminescent thermometry. In: Bünzli J-C, Pecharsky V, editors. Handbook on the Physics and Chemistry of Rare Earths. Vol. 49. Elsevier B.V; 2016. pp. 339-427. DOI: 10.1016/bs.hpcre.2016.03.005. ISSN: 0168-1273; ISBN: 9780444636997

[25] Rocha J, Brites CDS, Carlos LD. Lanthanide organic framework luminescent thermometers. Chemistry-A European Journal. 2016;**22**: 14782-14795. DOI: 10.1002/chem.201600860

[26] Runowski M, Woźny P, Martín IR. Optical pressure sensing in vacuum and high-pressure ranges using lanthanide-based luminescent thermometer-manometer. Journal of Materials Chemistry C. 2021;**9**:4643-4651. DOI: 10.1039/d1tc00709b

[27] Runowski M, Woźny P, Lavín V, Lis S. Optical pressure nano-sensor based on lanthanide doped SrB2O4:Sm2+ luminescence – novel high-pressure nanomanometer. Sensors and Actuators B: Chemical. 2018;**273**:585-591. DOI: 10.1016/j.snb.2018.06.089

[28] Goderski S, Runowski M, Woźny P, Lavín V, Lis S. Lanthanide upconverted luminescence for simultaneous contactless optical thermometry and manometry-sensing under extreme conditions of pressure and temperature. ACS Applied Materials & Interfaces. 2020;**12**:40475-40485. DOI: 10.1021/acsami.0c09882

[29] Antoniak MA, Zelewski SJ, Oliva R, Żak A, Kudrawiec R, Nyk M. Combined temperature and pressure sensing using luminescent NaBiF4:Yb,Er nanoparticles. ACS Applied Nano Materials. 2020;**3**:4209-4217. DOI: 10.1021/acsanm.0c00403

[30] Yan B. Luminescence response mode and chemical sensing mechanism for lanthanide-functionalized metal-organic framework hybrids. Inorganic Chemistry Frontiers. 2021;**8**:201-233

[31] Lakowicz JR. In: Lakowicz JR, editor. Principles of Fluorescence Spectroscopy. Boston, MA: Springer US; 2006

[32] Dutta A, Singh A, Wang X, Kumar A, Liu J. Luminescent sensing of nitroaromatics by crystalline porous materials. CrystEngComm. 2020;**22**: 7736-7781. DOI: 10.1039/d0ce01087a

[33] Förster T. Zwischenmolekulare energiewanderung und fluoreszenz. Annals of Physics. 1948;**437**:55-75. DOI: 10.1002/andp.19484370105

[34] Jones GA, Bradshaw DS. Resonance energy transfer: From fundamental theory to recent applications. Frontiers of Physics. 2019;**7**:1-19. DOI: 10.3389/fphy.2019.00100

[35] Dexter DL. A theory of sensitized luminescence in solids. The Journal of Chemical Physics. 1953;**21**:836-850. DOI: 10.1063/1.1699044

[36] Yamase, T.; 2001; pp. 187–203

[37] Fox MA. Photoinduced electron transfer. Photochemistry and Photobiology. 1990;**52**:617-627. DOI: 10.1111/j.1751-1097.1990.tb01808.x

[38] Huang XH, Shi L, Ying SM, Yan GY, Liu LH, Sun YQ, et al. Two lanthanide metal-organic frameworks as sensitive luminescent sensors for the detection of Cr2+ and Cr2O72- in aqueous solutions. CrystEngComm. 2018;**20**:189-197. DOI: 10.1039/c7ce01781b

[39] Zheng K, Liu Z, Jiang Y, Guo P, Li H, Zeng C, et al. Ultrahigh luminescence quantum yield lanthanide coordination polymer as a multifunctional sensor. Dalton Transactions. 2018;**47**: 17432-17440. DOI: 10.1039/c8dt03832e

[40] Sun Z, Yang M, Ma Y, Li L. Multi-responsive luminescent sensors based on two-dimensional lanthanide-metal organic frameworks for highly selective and sensitive detection of Cr (III) and Cr(VI) ions and benzaldehyde. Crystal Growth & Design. 2017;**17**: 4326-4335. DOI: 10.1021/acs.cgd.7b00638

[41] Li YX, Li SJ, Yan PF, Wang XY, Yao X, An GH, et al. Luminescence-colour-changing sensing of Mn2+ and Ag+ ions based on a white-light-emitting lanthanide coordination polymer. Chemical Communications. 2017;**53**:5067-5070. DOI: 10.1039/c7cc00258k

[42] Meng K, Yao C, Ma Q, Xue Z, Du Y, Liu W, et al. A reversibly responsive fluorochromic hydrogel based on lanthanide–mannose complex. Advancement of Science. 2019;**6**. DOI: 10.1002/advs.201802112. Article ID: 1802112

[43] Gu JZ, Cai Y, Liu Y, Liang XX, Kirillov AM. New lanthanide 2D coordination polymers constructed from a flexible ether-bridged tricarboxylate block: Synthesis, structures and luminescence sensing. Inorganica Chimica Acta. 2018;**469**:98-104. DOI: 10.1016/j.ica.2017.08.054

[44] Sun Z, Li Y, Ma Y, Li L. Dual-functional recyclable luminescent sensors based on 2D lanthanide-based metal-organic frameworks for highly sensitive detection of Fe^{3+} and 2,4-dinitrophenol. Dyes and Pigments. 2017; **146**:263-271. DOI: 10.1016/j.dyepig.2017.07.015

[45] Liu L, Wang Y, Lin R, Yao Z, Lin Q, Wang L, et al. Two water-stable lanthanide metal-organic frameworks with oxygen-rich channels for fluorescence sensing of Fe(Iii) ions in aqueous solution. Dalton Transactions. 2018;**47**:16190-16196. DOI: 10.1039/C8DT03741H

[46] Ma JJ, Liu WS. Effective luminescence sensing of Fe3+, Cr2O72-, MnO4- and 4-nitrophenol by lanthanide metal-organic frameworks with a new topology type. Dalton Transactions. 2019;**48**:12287-12295. DOI: 10.1039/c9dt01907c

[47] Feng X, Shang Y, Zhang H, Liu X, Wang X, Chen N, et al. Multi-functional lanthanide-CPs based on tricarboxylphenyl terpyridyl ligand as ratiometric luminescent thermometer and highly sensitive ion sensor with turn on/off effect. Dalton Transactions. 2020; **49**:4741-4750. DOI: 10.1039/d0dt00310g

[48] Jin J, Yang G, Liu Y, Cheng S, Liu J, Wu D, et al. Two series of microporous lanthanide-organic frameworks with different secondary building units and exposed lewis base active sites: Sensing, dye adsorption, and magnetic properties. Inorganic Chemistry. 2019;**58**:339-348. DOI: 10.1021/acs.inorgchem.8b02435

[49] Jing T, Chen L, Jiang F, Yang Y, Zhou K, Yu M, et al. Fabrication of a robust lanthanide metal-organic framework as a multifunctional material for Fe(III) detection, CO2 capture, and utilization. Crystal Growth & Design. 2018;**18**:2956-2963. DOI: 10.1021/acs.cgd.8b00068

[50] Li R, Qu XL, Zhang YH, Han HL, Li X. Lanthanide-organic frameworks constructed from naphthalenedisulfonates: Structure, luminescence and luminescence sensing properties. CrystEngComm. 2016;**18**: 5890-5900. DOI: 10.1039/c6ce01028h

[51] Li Y, Xu Y, Wang Y. Preparation and properties of transparent ultrathin lanthanide-complex films. Chemistry-A European Journal. 2016;**22**:10976-10982. DOI: 10.1002/chem.201601189

[52] Liu F, Gao W, Li P, Zhang XM, Liu JP. Lanthanide metal-organic frameworks as multifunctional luminescent sensor for detecting cations, anions and organic solvent molecules in aqueous solution. Journal of Solid State Chemistry. 2017;**253**:202-210. DOI: 10.1016/j.jssc.2017.05.040

[53] Ma L, Zhang Q, Wu H, Yang J, Liu YY, Ma JF. Multifunctional luminescence sensors assembled with lanthanide and a cyclotriveratrylene-based ligand. European Journal of Inorganic Chemistry. 2017;**2017**: 4221-4230. DOI: 10.1002/ejic.201700874

[54] Wang J, Yu M, Chen L, Li Z, Li S, Jiang F, et al. Construction of a stable lanthanide metal-organic framework as a luminescent probe for rapid naked-eye recognition of Fe^{3+} and acetone. Molecules. 2021;**26**:1695. DOI: 10.3390/molecules26061695

[55] Li GP, Liu G, Li YZ, Hou L, Wang YY, Zhu Z. Uncommon pyrazoyl-carboxyl bifunctional ligand-based microporous lanthanide systems: Sorption and luminescent sensing properties. Inorganic Chemistry. 2016;

55:3952-3959. DOI: 10.1021/acs.inorgchem.6b00217

[56] Wu YP, Xu GW, Dong WW, Zhao J, Li DS, Zhang J, et al. Anionic lanthanide MOFs as a platform for iron-selective sensing, systematic color tuning, and efficient nanoparticle catalysis. Inorganic Chemistry. 2017;**56**:1402-1411. DOI: 10.1021/acs.inorgchem.6b02476

[57] Yang D, Lu L, Feng S, Zhu M. First Ln-MOF as a trifunctional luminescent probe for the efficient sensing of aspartic acid, Fe3+and DMSO. Dalton Transactions. 2020;**49**:7514-7524. DOI: 10.1039/d0dt00938e

[58] Jia P, Wang Z, Zhang Y, Zhang D, Gao W, Su Y, et al. Selective sensing of Fe3+ ions in aqueous solution by a biodegradable platform based lanthanide metal organic framework. Spectrochimica Acta, Part A: Molecular and Biomolecular Spectroscopy. 2020:230. DOI: 10.1016/j.saa.2020.118084

[59] Abdelhamid HN, Bermejo-Gómez A, Martín-Matute B, Zou X. A water-stable lanthanide metal-organic framework for fluorimetric detection of ferric ions and tryptophan. Microchimica Acta. 2017; **184**:3363-3371. DOI: 10.1007/s00604-017-2306-0

[60] Fan B, Wei J, Ma X, Bu X, Xing N, Pan Y, et al. Synthesis of lanthanide-based room temperature ionic liquids with strong luminescence and selective sensing of Fe(III) over mixed metal ions. Industrial and Engineering Chemistry Research. 2016;**55**:2267-2271. DOI: 10.1021/acs.iecr.5b03947

[61] Li L, Chen Q, Niu Z, Zhou X, Yang T, Huang W. Lanthanide metal-organic frameworks assembled from a fluorene-based ligand: selective sensing of Pb2+ and Fe3+ Ions. Journal of Materials Chemistry C. 2016;**4**: 1900-1905. DOI: 10.1039/c5tc04320d

[62] Xu QW, Dong G, Cui R, Li X. 3D lanthanide-coordination frameworks constructed by a ternary mixed-ligand: Crystal structure, Luminescence and luminescence sensing. CrystEngComm. 2020;**22**:740-750. DOI: 10.1039/c9ce01779h

[63] Zhang H, Fan R, Chen W, Fan J, Dong Y, Song Y, et al. 3D lanthanide metal-organic frameworks based on mono-, tri-, and heterometallic tetranuclear clusters as highly selective and sensitive luminescent sensor for Fe3 + and Cu2+ ions. Crystal Growth & Design. 2016;**16**:5429-5440. DOI: 10.1021/acs.cgd.6b00903

[64] Wang KM, Du L, Ma YL, Zhao JS, Wang Q, Yan T, et al. Multifunctional chemical sensors and luminescent thermometers based on lanthanide metal-organic framework materials. CrystEngComm. 2016;**18**:2690-2700. DOI: 10.1039/c5ce02367j

[65] Xu H, Hu HC, Cao CS, Zhao B. Lanthanide organic framework as a regenerable luminescent probe for Fe3+. Inorganic Chemistry. 2015;**54**(10): 4585-4587. DOI: 10.1021/acs.inorgchem.5b00113

[66] Li JM, Huo R, Li X, Sun HL. Lanthanide-organic frameworks constructed from 2,7-Naphthalenedisulfonate and 1 H-Imidazo[4,5- f][1,10]-phenanthroline: Synthesis, structure, and luminescence with near-visible light excitation and magnetic properties. Inorganic Chemistry. 2019;**58**:9855-9865. DOI: 10.1021/acs.inorgchem.9b00925

[67] Wang D, Sun L, Hao C, Yan Y, Liang Z. Lanthanide metal-organic

frameworks based on a 1,2,3-Triazole-containing tricarboxylic acid ligand for luminescence sensing of metal ions and nitroaromatic compounds. RSC Advances. 2016;**6**:57828-57834. DOI: 10.1039/c6ra06303a

[68] Li ZJ, Li XY, Yan YT, Hou L, Zhang WY, Wang YY. Tunable emission and selective luminescence sensing in a series of lanthanide metal-organic frameworks with uncoordinated lewis basic triazolyl sites. Crystal Growth & Design. 2018;**18**:2031-2039. DOI: 10.1021/acs.cgd.7b01453

[69] Smith JA, Singh-Wilmot MA, Carter KP, Cahill CL, Ridenour JA. Lanthanide-2,3,5,6-tetrabromoterephthalic acid metal-organic frameworks: Evolution of halogen·halogen interactions across the lanthanide series and their potential as selective bifunctional sensors for the detection of Fe 3+, Cu 2+, and nitroaromatics. Crystal Growth & Design. 2019;**19**: 305-319. DOI: 10.1021/acs.cgd.8b01426

[70] Cao XM, Wei N, Liu L, Li L, Han ZB. Luminescent lanthanide-organic polyrotaxane framework as a turn-off sensor for nitrobenzene and Fe3+. RSC Advances. 2016;**6**:19459-19462. DOI: 10.1039/c5ra25872c

[71] Zhang X, Zhan Z, Liang X, Chen C, Liu X, Jia Y, et al. Lanthanide-MOFs constructed from mixed dicarboxylate ligands as selective multi-responsive luminescent sensors. Dalton Transactions. 2018;**47**:3272-3282. DOI: 10.1039/c7dt02966g

[72] Liu W, Huang X, Xu C, Chen C, Yang L, Dou W, et al. A multi-responsive regenerable europium–organic framework luminescent sensor for Fe3+, CrVIAnions, and picric acid. Chemistry—A European Journal. 2016;**22**: 18769-18776. DOI: 10.1002/chem.201603607

[73] Yan W, Zhang C, Chen S, Han L, Zheng H. Two lanthanide metal−organic frameworks as remarkably selective and sensitive bifunctional luminescence sensor for metal ions and small organic molecules. ACS Applied Materials & Interfaces. 2017;**9**:1629-1634. DOI: 10.1021/acsami.6b14563

[74] Zhang Q, Wang J, Kirillov AM, Dou W, Xu C, Xu C, et al. Multifunctional Ln-MOF luminescent probe for efficient sensing of Fe3+, Ce3+, and acetone. ACS Applied Materials & Interfaces. 2018;**10**:23976-23986. DOI: 10.1021/acsami.8b06103

[75] Wen RM, Han S, de Ren GJ, Chang Z, Li YW, Bu XH. A flexible zwitterion ligand based lanthanide metal-organic framework for luminescence sensing of metal ions and small molecules. Dalton Transactions. 2015;**44**:10914-10917. DOI: 10.1039/c4dt02445a

[76] Lu SQ, Liu YY, Duan ZM, Wang ZX, Li MX, He X. Improving water-stability and porosity of lanthanide metal-organic frameworks by stepwise synthesis for sensing and removal of heavy metal ions. Crystal Growth & Design. 2018;**18**: 4602-4610. DOI: 10.1021/acs.cgd.8b00575

[77] Mi X, Sheng D, Yu Y, Wang Y, Zhao L, Lu J, et al. Tunable light emission and multiresponsive luminescent sensitivities in aqueous solutions of two series of lanthanide metal-organic frameworks based on structurally related ligands. ACS Applied Materials & Interfaces. 2019;**11**: 7914-7926. DOI: 10.1021/acsami.8b18320

[78] Silva Lins IM, da Silva D, Fonseca J, Lourenço da Luz L, Chojnacki J, Júnior SA, et al. Novel luminescent calixarene-based lanthanide materials: From synthesis and characterization to the selective detection of Fe3+. Journal of Solid State Chemistry. 2021:295. DOI: 10.1016/j.jssc.2020.121916

[79] Zheng K, Lou KL, Zeng CH, Li SS, Nie ZW, Zhong S. Hybrid membrane of agarose and lanthanide coordination polymer: A selective and sensitive Fe3+ sensor. Photochemistry and Photobiology. 2015;**91**:814-818. DOI: 10.1111/php.12460

[80] Wang Y, Huang R, Zhang J, Cheng G, Yang H. Lanthanide(Tb3+, Eu3+)-functionalized a new one dimensional Zn-MOF composite as luminescent probe for highly selectively sensing Fe3+. Polyhedron. 2018;**148**:178-183. DOI: 10.1016/j.poly.2018.04.013

[81] Fan W, Du J, Kou J, Zhang Z, Liu F. Hierarchical porous cellulose/lanthanide hybrid materials as luminescent sensor. Journal of Rare Earths. 2018;**36**: 1036-1043. DOI: 10.1016/j.jre.2018.03.021

[82] Liang YT, Yang GP, Liu B, Yan YT, Xi ZP, Wang YY. Four super water-stable lanthanide-organic frameworks with active uncoordinated carboxylic and pyridyl groups for selective luminescence sensing of Fe3+. Dalton Transactions. 2015;**44**:13325-13330. DOI: 10.1039/c5dt01421b

[83] Zhao XL, Tian D, Gao Q, Sun HW, Xu J, Bu XH. A chiral lanthanide metal-organic framework for selective sensing of Fe(III) Ions. Dalton Transactions. 2016;**45**:1040-1046. DOI: 10.1039/c5dt03283k

[84] Ning Y, Wang L, Yang GP, Wu Y, Bai N, Zhang W, et al. Four new lanthanide-organic frameworks: Selective luminescent sensing and magnetic properties. Dalton Transactions. 2016;**45**:12800-12806. DOI: 10.1039/c6dt01393g

[85] Chen M, Xu WM, Tian JY, Cui H, Zhang JX, Liu C, et al. A Terbium(Iii) lanthanide-organic framework as a platform for a recyclable multi-responsive luminescent sensor. Journal of Materials Chemistry C. 2017;**5**: 2015-2021. DOI: 10.1039/C6TC05615F

[86] Liu LH, Qiu XT, Wang YJ, Shi Q, Sun YQ, Chen YP. NIR emission and luminescent sensing of a lanthanide-organic framework with lewis basic imidazole and pyridyl sites. Dalton Transactions. 2017;**46**:12106-12113. DOI: 10.1039/c7dt02745a

[87] Wang Y, Xing SH, Bai FY, Xing YH, Sun LX. Stable lanthanide-organic framework materials constructed by a triazolyl carboxylate ligand: Multifunction detection and white luminescence tuning. Inorganic Chemistry. 2018;**57**:12850-12859. DOI: 10.1021/acs.inorgchem.8b02050

[88] Shi D, Yang X, Ma Y, Niu M, Jones RA. Construction of 14-metal lanthanide nanorings with NIR luminescence response to ions. Chemical Communications. 2020;**56**:8651-8654. DOI: 10.1039/d0cc04242k

[89] Cui Z, Zhang X, Liu S, Zhou L, Li W, Zhang J. Anionic lanthanide metal-organic frameworks: Selective separation of cationic dyes, solvatochromic behavior, and luminescent sensing of Co (II) ion. Inorganic Chemistry. 2018;**57**: 11463-11473. DOI: 10.1021/acs.inorgchem.8b01319

[90] Li JJ, Fan TT, Qu XL, Han HL, Li X. Temperature-induced 1D lanthanide polymeric frameworks based on Lnn (n

= 2, 2, 4, 6) cores: Synthesis, crystal structures and luminescence properties. Dalton Transactions. 2016;**45**:2924-2935. DOI: 10.1039/c5dt04262c

[91] Lian X, Yan B. Novel core-shell structure microspheres based on lanthanide complexes for white-light emission and fluorescence sensing. Dalton Transactions. 2016;**45**:2666-2673. DOI: 10.1039/c5dt03939h

[92] Su R, Gao J, Deng S, Zhang R, Zheng Y. Dual-target optical sensors assembled by lanthanide complex incorporated sol–gel-derived polymeric films. Journal of Sol-Gel Science and Technology. 2016;**78**:606-612. DOI: 10.1007/s10971-016-3982-7

[93] Liang YY, Luo LJ, Li Y, Ling BK, Chen BW, Wang XW, et al. A luminescent probe for highly selective Cu2+ sensing using a lanthanide-doped metal organic framework with large pores. European Journal of Inorganic Chemistry. 2019; **2019**:206-211. DOI: 10.1002/ ejic.201800945

[94] Sun Z, Sun J, Xi L, Xie J, Wang X, Ma Y, et al. Two novel lanthanide metal-organic frameworks: Selective luminescent sensing for nitrobenzene, Cu2+, and MnO4. Crystal Growth & Design. 2020;**20**:5225-5234. DOI: 10.1021/acs.cgd.0c00432

[95] Huang P, Wu F, Mao L. Target-triggered switching on and off the luminescence of lanthanide coordination polymer nanoparticles for selective and sensitive sensing of copper ions in rat brain. Analytical Chemistry. 2015;**87**: 6834-6841. DOI: 10.1021/acs. analchem.5b01155

[96] Ma Q, Zhang M, Xu X, Meng K, Yao C, Zhao Y, et al. Multiresponsive supramolecular luminescent hydrogels based on a nucleoside/lanthanide complex. ACS Applied Materials & Interfaces. 2019;**11**:47404-47412. DOI: 10.1021/acsami.9b17236

[97] He J, Wang J, Xu Q, Wu X, Dutta A, Kumar A, et al. Syntheses and crystal structures of new dinuclear lanthanide complexes based on 3-(4-Hydroxyphenyl)Propanoic acid: Hirshfeld surface analyses and photoluminescence sensing. New Journal of Chemistry. 2019;**43**:13499-13508. DOI: 10.1039/c9nj02213a

[98] Xu Q, Li Z, Li H. Water-soluble luminescent hybrid composites consisting of oligosilsesquioxanes and lanthanide complexes and their sensing ability for Cu2+. Chemistry-A European Journal. 2016;**22**:3037-3043. DOI: 10.1002/chem.201504300

[99] Wang S, Cao T, Yan H, Li Y, Lu J, Ma R, et al. Functionalization of microporous lanthanide-based metal-organic frameworks by dicarboxylate ligands with methyl-substituted thieno [2,3-b]thiophene groups: Sensing activities and magnetic properties. Inorganic Chemistry. 2016;**55**: 5139-5151. DOI: 10.1021/acs. inorgchem.5b02801

[100] Mahmoud ME, Moussa Z, Prakasam T, Li L, Abiad MG, Patra D, et al. Lanthanides based metal organic frameworks for luminescence sensing of toxic metal ions. Journal of Solid State Chemistry. 2020;**281**. DOI: 10.1016/j. jssc.2019.121031. Article ID: 121031

[101] Liu B, Huang Y, Zhu X, Hao Y, Ding Y, Wei W, et al. Smart lanthanide coordination polymer fluorescence probe for mercury(II) determination. Analytica Chimica Acta. 2016;**912**: 139-145. DOI: 10.1016/j.aca.2016. 01.044

[102] Lin J, Cheng Q, Zhou J, Lin X, Reddy RCK, Yang T, et al. Five 3D lanthanide-based coordination polymers with 3,3,6T13 topology: Structures and luminescent sensor for Hg2+ and Pb2+ Ions. Journal of Solid State Chemistry. 2019;**270**:339-345. DOI: 10.1016/j.jssc.2018.11.033

[103] Ji G, Liu J, Gao X, Sun W, Wang J, Zhao S, et al. A luminescent lanthanide MOF for selectively and ultra-high sensitively detecting Pb2+ ions in aqueous solution. Journal of Materials Chemistry A. 2017;**5**:10200-10205. DOI: 10.1039/c7ta02439h

[104] Lian C, Chen Y, Li S, Hao MY, Gao F, Yang LR. Synthesis and characterization of lanthanide-based coordination polymers for highly selective and sensitive luminescent sensor for Pb2+over mixed metal ions. Journal of Alloys and Compounds. 2017; **702**:303-308. DOI: 10.1016/j.jallcom.2017.01.260

[105] Li B, Zhou J, Bai F, Xing Y. Lanthanide–organic framework based on a 4,4-(9,9-Dimethyl-9H-Fluorene-2,7-Diyl) dibenzoic acid: Synthesis, structure and fluorescent sensing for a variety of cations and anions simultaneously. Dyes and Pigments. 2020;**172**. DOI: 10.1016/j.dyepig.2019.107862. Article ID: 107862

[106] Ding B, Liu SX, Cheng Y, Guo C, Wu XX, Guo JH, et al. Heterometallic alkaline earth-lanthanide BaII-LaIII microporous metal-organic framework as bifunctional luminescent probes of Al3+ and MnO4. Inorganic Chemistry. 2016;**55**:4391-4402. DOI: 10.1021/acs.inorgchem.6b00111

[107] Zhang PF, Yang GP, Li GP, Yang F, Liu WN, Li JY, et al. Series of water-stable lanthanide metal-organic frameworks based on carboxylic acid imidazolium chloride: Tunable luminescent emission and sensing. Inorganic Chemistry. 2019;**58**: 13969-13978. DOI: 10.1021/acs.inorgchem.9b01954

[108] Liu G, Lu YK, Ma YY, Wang XQ, Hou L, Wang YY. Syntheses of three new isostructural lanthanide coordination polymers with tunable emission colours through bimetallic doping, and their luminescence sensing properties. Dalton Transactions. 2019; **48**:13607-13613. DOI: 10.1039/c9dt02733e

[109] Mondal TK, Mondal S, Ghorai UK, Saha SK. White light emitting lanthanide based carbon quantum dots as toxic Cr (VI) and PH sensor. Journal of Colloid and Interface Science. 2019;**553**:177-185. DOI: 10.1016/j.jcis.2019.06.009

[110] Zou JY, Li L, You SY, Cui HM, Liu YW, Chen KH, et al. Sensitive luminescent probes of aniline, benzaldehyde and Cr(VI) based on a Zinc(II) metal-organic framework and its lanthanide(III) post-functionalizations. Dyes and Pigments. 2018;**159**:429-438. DOI: 10.1016/j.dyepig.2018.07.005

[111] Dang H, Li Y, Zou H, Liu S. Tunable white-light emission hybrids based on lanthanide complex functionalized poly (ionic liquid): Assembly and chemical sensing. Dyes and Pigments. 2020;**172**. DOI: 10.1016/j.dyepig.2019.107804. Article ID: 107804

[112] Chen W, Fan R, Fan J, Liu H, Sun T, Wang P, et al. Lanthanide coordination polymer-based composite films for selective and highly sensitive detection of Cr2O72- in aqueous media. Inorganic Chemistry. 2019;**58**(22):15118–15125. DOI: 10.1021/acs.inorgchem.9b01841

[113] Zhou Z, Gu J, Qiao X, Wu H, Fu H, Wang L, et al. Double protected

lanthanide fluorescence core@shell colloidal hybrid for the selective and sensitive detection of ClO. Sensors and Actuators B: Chemical. 2019;**282**: 437-442. DOI: 10.1016/j.snb.2018.11.103

[114] Bradberry SJ, Byrne JP, McCoy CP, Gunnlaugsson T. Lanthanide luminescent logic gate mimics in soft matter: [H+] and [F-] dual-input device in a polymer gel with potential for selective component release. Chemical Communications. 2015;**51**:16565-16568. DOI: 10.1039/c5cc05009j

[115] Xu W, Zhou Y, Huang D, Su M, Wang K, Xiang M, et al. Luminescent sensing profiles based on anion-responsive lanthanide(iii) quinolinecarboxylate materials: Solid-state structures, photophysical properties, and anionic species recognition. Journal of Materials Chemistry C. 2015;**3**:2003-2015. DOI: 10.1039/c4tc02369b

[116] Liu X, Yang X, Ma Y, Liu J, Shi D, Niu M, et al. Construction of two lanthanide schiff base complexes: Chiral "Triple-Decker" structure and NIR luminescent response towards anions. Journal of Luminescence. 2021;**229**. DOI: 10.1016/j.jlumin.2020.117679. Article ID: 117679

[117] Sun Z, Hu P, Ma Y, Li L. Lanthanide organic frameworks for luminescence sensing of nitrobenzene and nitrophenol with high selectivity. Dyes and Pigments. 2017;**143**:10-17. DOI: 10.1016/j.dyepig.2017.04.015

[118] Khullar S, Singh S, Das P, Mandal SK. Luminescent lanthanide-based probes for the detection of nitroaromatic compounds in water. ACS Omega. 2019;**4**:5283-5292. DOI: 10.1021/acsomega.9b00223

[119] Zhao SN, Song XZ, Zhu M, Meng X, Wu LL, Song SY, et al. Highly thermostable lanthanide metal-organic frameworks exhibiting unique selectivity for nitro explosives. RSC Advances. 2015;**5**:93-98. DOI: 10.1039/c4ra13773f

[120] Wang X, Zhang L, Yang J, Liu F, Dai F, Wang R, et al. Lanthanide metal-organic frameworks containing a novel flexible ligand for luminescence sensing of small organic molecules and selective adsorption. Journal of Materials Chemistry A. 2015;**3**:12777-12785. DOI: 10.1039/c5ta00061k

[121] Yang LZ, Wang J, Kirillov AM, Dou W, Xu C, Fang R, et al. 2D lanthanide MOFs driven by a Rigid 3,5-Bis(3-Carboxy-Phenyl)pyridine building block: Solvothermal syntheses, structural features, and photoluminescence and sensing properties. CrystEngComm. 2016;**18**:6425-6436. DOI: 10.1039/c6ce00885b

[122] Einkauf JD, Ortega RE, Mathivathanan L, De Lill DT. Nitroaromatic sensing with a new lanthanide coordination polymer [Er2(C10H4O4S2)3(H2O)6]:N assembled by 2,2′-Bithiophene-5,5′-Dicarboxylate. New Journal of Chemistry. 2017;**41**: 10929-10934. DOI: 10.1039/c7nj01677h

[123] Liu W, Huang X, Chen C, Xu C, Ma J, Yang L, et al. Function-oriented: The construction of lanthanide MOF luminescent sensors containing dual-function urea hydrogen-bond sites for efficient detection of picric acid. Chemistry—A European Journal. 2019; **25**:1090-1097. DOI: 10.1002/chem.201805080

[124] Wang JM, Zhang PF, Cheng JG, Wang Y, Ma LL, Yang GP, et al. Luminescence tuning and sensing properties of stable 2D lanthanide metal-organic frameworks built with

symmetrical flexible tricarboxylic acid ligands containing ether oxygen bonds. CrystEngComm. 2021;**23**:411-418. DOI: 10.1039/d0ce01528h

[125] Moscoso FG, Almeida J, Sousaraei A, Lopes-Costa T, Silva AMG, Cabanillas-Gonzalez J, et al. A lanthanide MOF immobilized in PMMA transparent films as a selective fluorescence sensor for nitroaromatic explosive vapours. Journal of Materials Chemistry C. 2020; **8**:3626-3630. DOI: 10.1039/d0tc00376j

[126] Fu R, Hu S, Wu X. Rapid and sensitive detection of nitroaromatic explosives by using new 3D lanthanide phosphonates. Journal of Materials Chemistry A. 2017;**5**:1952-1956. DOI: 10.1039/c6ta10152f

[127] Li XZ, Zhou LP, Yan LL, Yuan DQ, Lin CS, Sun QF. Evolution of luminescent supramolecular lanthanide M2nL3n complexes from helicates and tetrahedra to cubes. Journal of the American Chemical Society. 2017; **139**:8237-8244. DOI: 10.1021/jacs.7b02764

[128] Zhang F, Chen S, Nie S, Luo J, Lin S, Wang Y, et al. Waste PET as a Reactant for Lanthanide MOF Synthesis and Application in Sensing of Picric Acid. Polymers. 2019;**11**:2015. DOI: 10.3390/polym11122015

[129] Raizada M, Sama F, Ashafaq M, Shahid M, Khalid M, Ahmad M, et al. Synthesis, structure and magnetic studies of lanthanide metal–organic frameworks (Ln–MOFs): Aqueous phase highly selective sensors for picric acid as well as the arsenic ion. Polyhedron. 2018; **139**:131-141. DOI: 10.1016/j.poly.2017.09.052

[130] Wang X, Yan P, Li Y, An G, Yao X, Li G. Highly efficient white-light emission and UV-Visible/NIR luminescence sensing of lanthanide metal-organic frameworks. Crystal Growth & Design. 2017;**17**: 2178-2185. DOI: 10.1021/acs.cgd.7b00112

[131] Shi Y, Wang WM, Tang GP, Zhang YX, Li M, Wu ZL. Robust lanthanide metal–organic frameworks with highly sensitive sensing of aniline and slow magnetization relaxation behaviors. Polyhedron. 2018;**153**:122-127. DOI: 10.1016/j.poly.2018.07.003

[132] Shi B, Zhong Y, Guo L, Li G. Two dimethylphenyl imidazole dicarboxylate-based lanthanide metal-organic frameworks for luminescence sensing of benzaldehyde. Dalton Transactions. 2015;**44**:4362-4369. DOI: 10.1039/c4dt03326d

[133] Han Y, Yan P, Sun J, An G, Yao X, Li Y, et al. Luminescence and white-light emitting luminescent sensor of tetrafluoroterephthalate-lanthanide metal-organic frameworks. Dalton Transactions. 2017;**46**:4642-4653. DOI: 10.1039/c7dt00215g

[134] Yao X, Wang X, Han Y, Yan P, Li Y, Li G. Structure, color-tunable luminescence, and UV-Vis/NIR benzaldehyde detection of lanthanide coordination polymers based on two fluorinated ligands. CrystEngComm. 2018;**20**:3335-3343. DOI: 10.1039/c8ce00516h

[135] Wang L, Fan G, Xu X, Chen D, Wang L, Shi W, et al. Detection of polychlorinated benzenes (persistent organic pollutants) by a luminescent sensor based on a lanthanide metal-organic framework. Journal of Materials Chemistry A. 2017;**5**:5541-5549. DOI: 10.1039/c7ta00256d

[136] Zhu Y, Wang L, Chen X, Wang P, Fan Y, Zhang P. 3D lanthanide metal-organic frameworks constructed from 2,6-naphthalenedicarboxylate ligand: Synthesis, structure, luminescence and dye adsorption. Journal of Solid State Chemistry. 2017;**251**:248-254. DOI: 10.1016/j.jssc.2017.04.026

[137] Du N, Gao X, Song J, Wang ZN, Xing YH, Bai FY, et al. Optical detection of small biomolecule thiamines at a micromolar level by highly luminescent lanthanide complexes with tridentate N-heterocyclic ligands. RSC Advances. 2016;**6**:71012-71024. DOI: 10.1039/c6ra10869e

[138] Wang Y, Du N, Zhang X, Wang Y, Xing YH, Bai FY, et al. Functional sensing materials based on lanthanide N-heterocyclic polycarboxylate crystal frameworks for detecting thiamines. Crystal Growth & Design. 2018;**18**: 2259-2269. DOI: 10.1021/acs.cgd.7b01684

[139] Lian X, Yan B. A lanthanide metal-organic framework (MOF-76) for adsorbing dyes and fluorescence detecting aromatic pollutants. RSC Advances. 2016;**6**:11570-11576. DOI: 10.1039/c5ra23681a

[140] Zhang WW, Wang YL, Liu Q, Liu QY. Lanthanide-benzophenone-3,3′-Disulfonyl-4,4′-dicarboxylate frameworks: Temperature and 1-hydroxypyren luminescence sensing and proton conduction. Inorganic Chemistry. 2018;**57**:7805-7814. DOI: 10.1021/acs.inorgchem.8b00865

[141] Singha DK, Majee P, Mondal SK, Mahata P. Detection of pesticide using the large stokes shift of luminescence of a mixed lanthanide co-doped metal–organic framework. Polyhedron. 2019; **158**:277-282. DOI: 10.1016/j.poly.2018.10.066

[142] Ren K, Wu SH, Guo XF, Wang H. Lanthanide organic framework as a reversible luminescent sensor for sulfamethazine antibiotics. Inorganic Chemistry. 2019;**58**:4223-4229. DOI: 10.1021/acs.inorgchem.8b03284

[143] Zhang F, Yao H, Chu T, Zhang G, Wang Y, Yang Y. A lanthanide MOF thin-film fixed with Co3O4 nano-anchors as a highly efficient luminescent sensor for nitrofuran antibiotics. Chemistry—A European Journal. 2017; **23**:10293-10300. DOI: 10.1002/chem.201701852

[144] Wu S, Zhu M, Zhang Y, Kosinova M, Fedin VP, Gao E. Luminescent sensors based on coordination polymers with adjustable emissions for detecting biomarker of pollutant ethylbenzene and styrene. Applied Organometallic Chemistry. 2021;**35**:e6058. DOI: 10.1002/aoc.6058

[145] Belousov YA, Drozdov AA, Taydakov IV, Marchetti F, Pettinari R, Pettinari C. Lanthanide azolecarboxylate compounds: Structure, luminescent properties and applications. Coordination Chemistry Reviews. 2021; **445**:214084. DOI: 10.1016/j.ccr.2021.214084